

# Influence of reducing reagent combination in graphene oxide reduction

Chengyuan Hu, Rong Zhou, Chuanjie Fan, Xiaodong Zhou

State Key Laboratory of Chemical Engineering, East China University of Science and Technology, Shanghai 200237, People's Republic of China  
E-mail: xdzhou@ecust.edu.cn

Published in Micro & Nano Letters; Received on 17th July 2015; Revised on 14th September 2015; Accepted on 15th September 2015

Large-scale production of high-quality graphene nanosheets has been considered to be an interesting and significant challenge. A new approach is reported regarding the fabrication of high-quality graphene nanosheets via chemical reduction with the combination of reducing reagents from graphene oxide (GO). High-conducting reduced GO (RGO) was provided with the combination of hydrazine hydrate and hydroiodic acid. RGO was characterised by X-ray diffraction, Fourier-transform infrared spectroscopy, X-ray photoelectron spectroscopy, Raman, thermo gravimetric analysis, atomic force microscopy and four-probe conductivity tester. Characterisation results indicated that oxygenated functional groups were removed from GO, and high graphitisation has occurred in GO reduction process. The electrical conductivity of RGO was considerably improved and the C/O ratio of RGO was higher than that prepared by single reducing reagent. Combination of hydrate hydrazine and hydroiodic acid have showed high reduction efficiency and good synergistic effect in GO reduction process. The findings in this work can promote research on prepared graphene-based nanosheets composites by a quick and effective processing technique.

**1. Introduction:** Andre K. Geim and Kostya S. Novoselov exfoliated graphene by a ‘very simple’ way which used the scotch tape to peel off highly ordered pyrolytic graphite [1]. Recently, it has reported that graphene has numerous excellent performances such as high electron mobility, high thermal conductivity, hardest material, huge specific surface area and so on [2–5]. Lots of attention has been paid to the production of high-quality graphene nanosheets in large scale due to its excellent performance and potential application in various fields.

There are many methods to prepare graphene nanosheets, including mechanical stripping [1], chemical vapour deposition [6], chemical oxidation reduction [7] and others [8–12]. The chemical oxidation reduction method has been considered as an ideal way to prepare superior and high-conductive graphene in large scale for its relatively simple process, low cost and high yields. It has been introduced to prepare graphene from graphene oxide (GO). Reducing reagent is the crucial factor in the GO reduction process since it is directly related with graphene quality. Until now, chemical oxidation reduction process of GO has been involved in the use of hydrazine hydrate ( $\text{N}_2\text{H}_4\cdot\text{H}_2\text{O}$ ) [7], hydroiodic acid (HI) [13], sodium borohydride ( $\text{NaBH}_4$ ) [14], ammonia ( $\text{NH}_3\cdot\text{H}_2\text{O}$ ) [15], glucose [16], vitamin C [17, 18] and others.

However, single reducing reagent gave rise to high sheet resistance of reduced GO (RGO) and the electrical conductivity of RGO cannot be fully restored. Oxygenated functional groups in GO cannot be removed completely, which resulted in the incomplete reduction of GO [7, 13–18]. Therefore, it is essential to find out an excellent and convenient way to restore graphene structure which is suitable for mass production of high-quality RGO. GO reduction process is the deprivation of oxygenated functional groups and reestablishment of  $\pi$ - $\pi$  conjugated structure from pristine graphite. Different reducing reagents have different removal ability on the various oxygenated functional groups of GO. It has reported that hydrazine hydrate can reduce hydroxyl group more effectively than other oxygenated functional groups [7] and HI can replace epoxy functional group with iodide, which is good leaving groups, to produce RGO [13].

As we know, synergistic effect was applied in many chemical reaction processes, such as combination of catalyser in the catalytic reaction and nucleating agent in the polymer synthesis process. We expect that synergistic effect can play an important role in

GO reduction process. Therefore, we employ combination of hydrazine hydrate and HI (first add hydrazine hydrate and then add HI) to reduce GO to prepare high-quality graphene and expect that the combination of reducing reagent could present good synergistic effect in the reduction process to prepare high-quality graphene.

In this Letter, we synthesised graphene through combination of hydrazine hydrate and HI, and then compared with RGOs reduced by hydrazine hydrate, HI, and combination of HI and hydrazine hydrate (first add HI and then add hydrazine hydrate), respectively. RGOs, which were reduced by four reducing reagents, were characterised by X-ray diffraction (XRD), Fourier-transform infrared (FTIR), X-ray photoelectron spectroscopy (XPS), Raman, thermo gravimetric analysis (TGA), atomic force microscopy (AFM) and electrical conductivity tester. This novel approach may be used for the fabrication and processing of high-quality RGO in large quantity.

## 2. Experimental sections

**2.1. Materials:** Flake graphite powder (200 mesh) was purchased from Shanghai Yifan Graphite Co., Ltd. Potassium permanganate ( $\text{KMnO}_4$ ), concentrated sulphuric acid ( $\text{H}_2\text{SO}_4$ , 98%), sodium nitrate ( $\text{NaNO}_3$ ), hydrogen peroxide ( $\text{H}_2\text{O}_2$ , 30 wt%) and hydrochloric acid (HCl, 36.5 wt%) were obtained from Sinopharm Chemical Reagent Co., Ltd. Hydrazine hydrate ( $\text{N}_2\text{H}_4\cdot\text{H}_2\text{O}$ , 35 wt%) and HI were acquired from Shanghai Lingfeng Chemical Reagent Co., Ltd. All the chemicals used in this research were of analytical pure grade.

High-speed shearing machine (F200) was purchased from Fluko Shanghai Instrument Co., Ltd (China). The ultrasound instrument was carried out on special equipment (20 kHz, 300 W) with a direct immersion probe of titanium alloy from Zhejiang Chenggong Ultrasonic Instrument Co., Ltd (China).

**2.2. Methods:** Graphite oxide was prepared from flake graphite powder by modified Hummers method with  $\text{H}_2\text{SO}_4$ ,  $\text{NaNO}_3$  and  $\text{KMnO}_4$  [19, 20]. It was reported that GO was reduced to graphene much easier than graphite oxide [21]. GO was obtained from graphite oxide with high-speed shearing machine and ultrasonic instrument.

2.2.1. Preparation of graphite oxide: About 5 g graphite and 2.3 g  $\text{NaNO}_3$  were added to 115 ml concentrated sulphuric acid with an ice bath, 15 g  $\text{KMnO}_4$  was added to the suspension slowly and a continuous intense stirring was kept for 2 h. The ice bath was removed and the suspension was heated up to 35 °C. After 2 h, 460 ml distilled water was added into the suspension slowly, the temperature was heated up to 95 °C and maintained for 30 min.  $\text{H}_2\text{O}_2$  was added into the suspension to remove the residual  $\text{KMnO}_4$ . After settled for 24 h, the suspension was centrifuged for five times and then added HCl and distilled water to wash the residual ion. Graphite oxide was freeze dried for 24 h and kept in the vacuum dryer.

2.2.2. Preparation of GO: About 0.1 g graphite oxide was dispersed in 100 ml distilled water, and treated with high-speed shearing machine at 10 000 rpm for 1 h to prepare a distributed evenly brown dispersion ( $1 \text{ mg ml}^{-1}$ ). This dispersion was treated with ultrasonic instrument for 2 h to prepare a yellow homogeneous GO suspension.

2.2.3. Preparation of RGO: RGO was, respectively, prepared from GO with four reducing reagents: hydrazine hydrate, HI, combination of hydrazine hydrate and HI, combination of HI and hydrazine hydrate.

About 1 ml hydrazine hydrate was added into 100 ml GO dispersion ( $1 \text{ mg ml}^{-1}$ ) and the mixture was kept at 95 °C with constant stirring for 24 h. The product was isolated by filtration, washed with acetone ( $2 \times 100 \text{ ml}$ ) and distilled water ( $5 \times 100 \text{ ml}$ ), and then was dried in a freeze dryer at  $-80 \text{ °C}$  for 24 h to yield RGO-1 powder.

RGO-2 was reduced from 100 ml GO dispersion ( $1 \text{ mg ml}^{-1}$ ) by adding 2 ml HI acid at 95 °C for 5 h. RGO-3 was reduced from 100 ml GO dispersion ( $1 \text{ mg ml}^{-1}$ ) by adding 1 ml hydrazine hydrate at 95 °C for 24 h first and then adding 2 ml HI acid at 95 °C for 5 h. RGO-4 was reduced from 100 ml GO dispersion ( $1 \text{ mg ml}^{-1}$ ) by adding 20 ml HI acid at 95 °C for 5 h first and then adding 10 ml hydrazine hydrate at 95 °C for 24 h. Four RGOs products were thus obtained.

2.3. Characterisation techniques: Powder XRD patterns were recorded on a D/max 2550 V instrument using  $\text{Cu-K}\alpha$  radiation from Rigaku Corporation (Japan). FTIR spectra (KBr) were collected using FTIR spectrometer (Nicolet 6700) from Thermo Fisher Scientific (America). All XPS measurements were taken in a Falion 60S instrument from EDAX company (America) using a monochromatic  $\text{Al-K}\alpha$  X-ray source at 100 W. Here, a monochromatic X-ray beam source at 1486.6 eV (aluminium anode) and 14 kV was used to scan upon the sample surface. A high flux X-ray source with aluminium anode was used for X-ray generation, and a quartz crystal monochromator was used to focus and scan the X-ray beam on the sample. Raman spectroscopy measurements were taken using a micro-Raman system (inVia + ReFlx) from Renishaw (UK) with laser frequency of 514 nm as excitation source (excitation energy: 2.41 eV), laser spot size was 1  $\mu\text{m}$  and power at the sample was below 10 mW, in order to avoid laser-induced heating. The thermal properties of graphene platelets were characterised by thermo gravimetric analyser (STA449C/3/G) from Netzsch-Geratebau GmbH (Germany). All RGO sample measurements were taken at a nitrogen gas flow rate of  $40 \text{ ml min}^{-1}$  over a temperature range of room temperature to 800 °C with a ramp rate of  $10 \text{ °C min}^{-1}$ . GO sample was also heated from room temperature to 800 °C at  $1 \text{ °C min}^{-1}$  to avoid thermal expansion of the GO due to rapid heating. GO and RGO monolayers were characterised by AFM (Agilent Technologies, Agilent 5500 AFM/SPM System) in a tapping mode. The electrical conductivities of GO and RGO were measured by using a four-probe conductivity tester (RTS-8 instrument) from Guangzhou 4-probes Technology Company

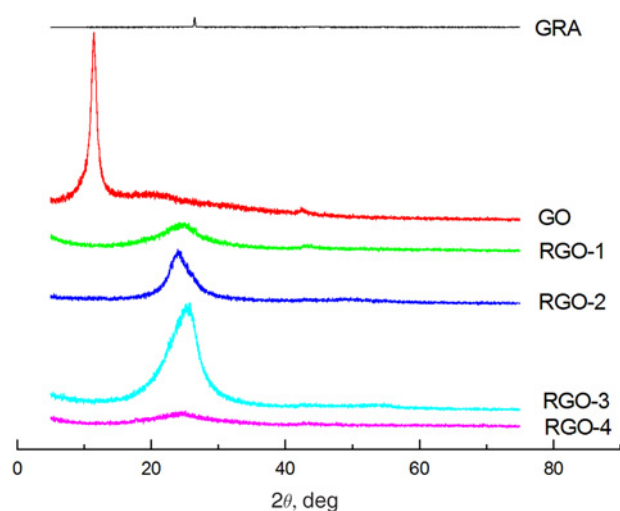


Fig. 1 XRD patterns of graphite (GRA), GO, RGO-1, RGO-2, RGO-3 and RGO-4

(China) at room temperature after pressing the samples into pellet form.

**3. Results and discussion:** The yellow homogeneous GO suspension was turned black after reducing with the reducing reagent indicating that reduction of GO has been occurred.

3.1. X-ray diffraction: As shown in Fig. 1, the powder XRD pattern of graphite, GO and RGOs were measured to research graphite crystal structure.

The XRD pattern of graphite exhibits only one intense peak centred at  $26.4^\circ$  while the interlayer distance of graphite is 0.335 nm. As graphite been oxidised to GO, the peak was shifted to  $11.4^\circ$  and interlayer distance of GO increased to 0.778 nm. The oxidation process of graphite leads to numerous oxygenated functional groups including hydroxyl group, carboxyl group, epoxy group and others [22]. Oxygenated functional groups have entered into the interlamination of graphite and expanded the interlayer distance of graphite.

Compared with GO pattern, the peak in RGO pattern which was shifted to about  $25^\circ$  obviously reveal that GO was reduced to RGO. As XRD pattern shows, peaks of RGO-1, RGO-2, RGO-3 and RGO-4 were shifted back to  $25^\circ$ ,  $24.1^\circ$ ,  $25.4^\circ$  and  $25^\circ$ , the interlayer distance decreased to about 0.356, 0.369, 0.351 and 0.356 nm, respectively. The interlayer distance of RGO has decreased for oxygenated functional groups between GO layers that have been removed in the reduction process, which was confirming the recovery of graphite crystal structure and the rebuilding of C–C bond skeleton structure [22].

The characteristic peak of RGO-3 was higher and narrower than that of other RGOs indicating that RGO-3 was well ordered with two-dimensional (2D) sheets and there was a decrease in the average interlayer spacing of RGO platelets. The interlayer distance of RGO-3 decreased more than other three RGO's due to more oxygenated functional groups have been removed in reduction process. The combination of hydrazine hydrate and HI has shown higher reducing ability than single reducing reagent.

3.2. Fourier-transform infrared: The FTIR spectra of GO and RGOs in Fig. 2 were measured to study the oxygenated functional groups in GO reduction process. The broad and intense peak of GO pattern in the frequency range of  $3400 \text{ cm}^{-1}$  is attributable to  $-\text{OH}$  bond of bound water in GO interlamination. The strong absorption peak at  $1730 \text{ cm}^{-1}$  is C=O bond of carboxylic acid and carbonyl moieties. The absorption peaks

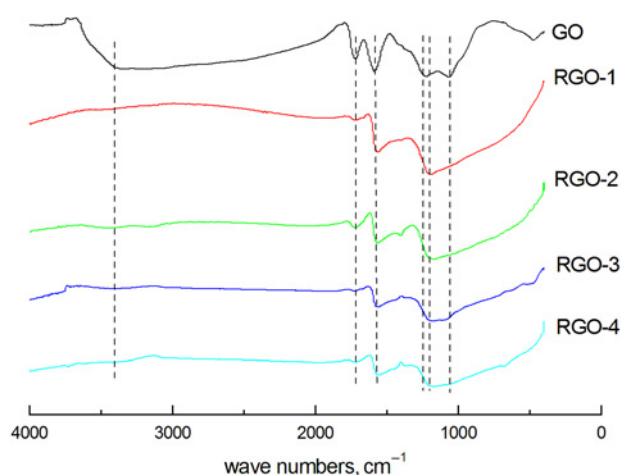


Fig. 2 FTIR spectra of GO, RGO-1, RGO-2, RGO-3 and RGO-4

located at 1570, 1220 and 1060  $\text{cm}^{-1}$  are ascribed to the C=C stretching deformation of the quinoid ring, the C–O–C (epoxy) bond of epoxy group and the C–O (alkoxy) stretching, respectively.

As shown in FTIR spectra of RGO, all the peaks due to oxygenated functional groups has decreased in intensity or disappeared indicating that the reduction process of GO to RGO nanosheets has occurred. The peak at 3400  $\text{cm}^{-1}$  has disappeared due to the bound water in GO interlamination has been removed. The C=O peak at 1730  $\text{cm}^{-1}$ , the C=C peak at 1570  $\text{cm}^{-1}$ , the C–O–C peak at 1178  $\text{cm}^{-1}$  and the C–O peak at 1060  $\text{cm}^{-1}$  have decreased in intensity, some of them disappeared entirely. The RGO-3 pattern showed that the peak of oxygenated functional groups has decreased much more than others in intensity and most of them disappeared entirely. This meant oxygenated functional groups have been removed in RGO-3 much more than that in other RGOs.

**3.3. X-ray photoelectron spectroscopy:** The C1s XPS spectra of graphite, GO and RGOs have been shown in Figs. 3a–f. High-resolution C1s peaks in XPS spectra of RGO proved that oxygenated functional groups have been removed.

There was only one peak at 284.4 eV due to C–C bond in Fig. 3a of graphite XPS spectra. The XPS peaks of GO at 284.4 eV in Fig. 3b assigned to C were one main C–C, one large C–O components and other two small C–O components, which were observed in the C1s peaks of the GO: C–C (284.4 eV) for  $\text{sp}^2$  carbon in graphite; C–O (286.3 eV); C=O (287.5 eV); O=C–O (289.1 eV).

As shown in Figs. 3c–f, the XPS peaks of all RGOs at 284.4 eV assigned to C were one main C–C and two small C–O components, which were observed in the C1s peaks of the RGO-1: C–C (284.4 eV) for  $\text{sp}^2$  carbon in graphite; C–O (286.4 eV); C=O (287.8 eV). C1s peaks of the RGO-2: C–C (284.4 eV) for  $\text{sp}^2$  carbon in graphite; C–O (286.5 eV); C=O (288.3 eV). C1s peaks of the RGO-3: C–C (284.4 eV) for  $\text{sp}^2$  carbon in graphite; C–O (286.5 eV); C=O (288.3 eV). C1s peaks of the RGO-4: C–C (284.4 eV) for  $\text{sp}^2$  carbon in graphite; C–O (286.8 eV); C=O (288.0 eV). The peak of O=C–O group disappeared, and the peak intensity of C–O and C=O decreased meant that most of oxygenated functional groups were removed in the reduction process.

The atomic ratio of carbon to oxygen (area of the C1s peak divided by area of the O1s peak) was calculated from the XPS survey spectrum after each treatment and the calculated results were shown in Table 1.

The value of atomic ratio (C1s/O1s) decreased when graphite was oxidised to GO due to lots of oxygenated functional groups were introduced; the value of atomic ratio (C1s/O1s) increased when GO was reduced to RGO since oxygenated functional groups were removed by reducing reagents. The atomic ratio

(C1s/O1s) of RGO-3 was larger than other RGO's meant that less oxygenated functional groups were remained in RGO-3 and most of them have been reduced by the combination of hydrazine hydrate and HI.

**3.4. Raman:** Raman spectra of graphite, GO and RGOs were provided in Fig. 4. As shown in Raman spectra of graphite, the band at 1584.1  $\text{cm}^{-1}$  was named as 'G band' and the other band at 1353.5  $\text{cm}^{-1}$  was named as 'D band' [23]. The G band was due to the first-order scattering of  $E_{2g}$  mode and D band was associated with the defects in graphite lattice, which was evidence for the presence of defects in graphite material such as bond-angle disorder, bond-length disorder, vacancies, edge defects and so on [24].

Raman spectra of GO possessed G band at 1602.4  $\text{cm}^{-1}$  and D band at 1358.1  $\text{cm}^{-1}$ . Compared with graphite, G band in GO was shifted towards higher wave number and D band was shifted to lower wave number which was due to the presence of isolated double bonds that resonate at frequencies higher than that of G band in graphite [24]. G band of all RGO appeared around 1584  $\text{cm}^{-1}$  meant the defect in carbon hexagonal network structure has been repaired by reducing reagent in GO reduction process.

The intensity ratio of G band to D band was used to measure the average crystallite size of the  $\text{sp}^2$  domains and estimate the disorder degree of graphite materials [24]. Oxygenated functional groups have been removed by chemical reduction, and the conjugated G network ( $\text{sp}^2$  carbon) would be re-established. However, the size of the re-established G network was smaller than the pristine one, which would consequently lead to an increase in the  $I_D/I_G$  ratio (Table 2).

Compared with GO, the  $I_D/I_G$  ratio of RGO has increased, indicating that the reduction process has altered the structure of GO with a large quantity of structural defects. The  $I_D/I_G$  ratio of RGO-3 is higher than other RGOs; and the crystallite size of  $\text{sp}^2$  carbon is smaller. That is because the reduction process of RGO-3 is much more thorough than other RGOs by the combination of hydrazine hydrate and HI.

The intensity of the 2D ( $\sim 2690 \text{ cm}^{-1}$ ) peak in RGO-3 Raman spectra increased much more than that of other RGOs, showing better graphitisation due to the better reduction process in RGO-3 [25].

**3.5. Thermo gravimetric analysis:** TGA was used to further assess the reduction degree of GO. Fig. 5 displays the TGA thermograms that showed weight loss as a function of temperature for GO (at a heating rate of 1  $^\circ\text{C min}^{-1}$ ; higher heating rates can cause GO to rapidly expand) and RGOs (at a heating rate of 10  $^\circ\text{C min}^{-1}$ ) under a nitrogen atmosphere.

As shown in TGA spectra, the pristine graphite was decomposed under 700  $^\circ\text{C}$  while GO was decomposed at 550  $^\circ\text{C}$ , with a 9.41% weight loss under 110  $^\circ\text{C}$  due to the bound water in GO interlamination was removed and a 22.17% weight loss between 150 and 250  $^\circ\text{C}$  owing to oxygenated functional groups were partly thermal decomposition to CO, CO<sub>2</sub> and H<sub>2</sub>O [26]. Distinctly different from the curves of GO, there was no obvious mass decrease between 150 and 250  $^\circ\text{C}$  in RGO TGA spectra that meant most of oxygenated functional groups have been removed in GO reduction process.

The decomposition temperatures of RGO-1, RGO-2, RGO-3 and RGO-4 were about 490, 580, 580 and 530  $^\circ\text{C}$ , respectively. However, there was a 13.88% weight loss between 150 and 250  $^\circ\text{C}$  in RGO-2 TGA spectra. When GO was reduced to RGO, a little of oxygenated functional groups was residual and most of them were removed, the  $\pi$ - $\pi$  conjugation has been repaired. The thermal stability of carbon skeleton has been recovered. RGO-3 showed higher thermal stability than other RGOs because of the better graphitisation and de-oxygenation of RGO-3 with enhanced

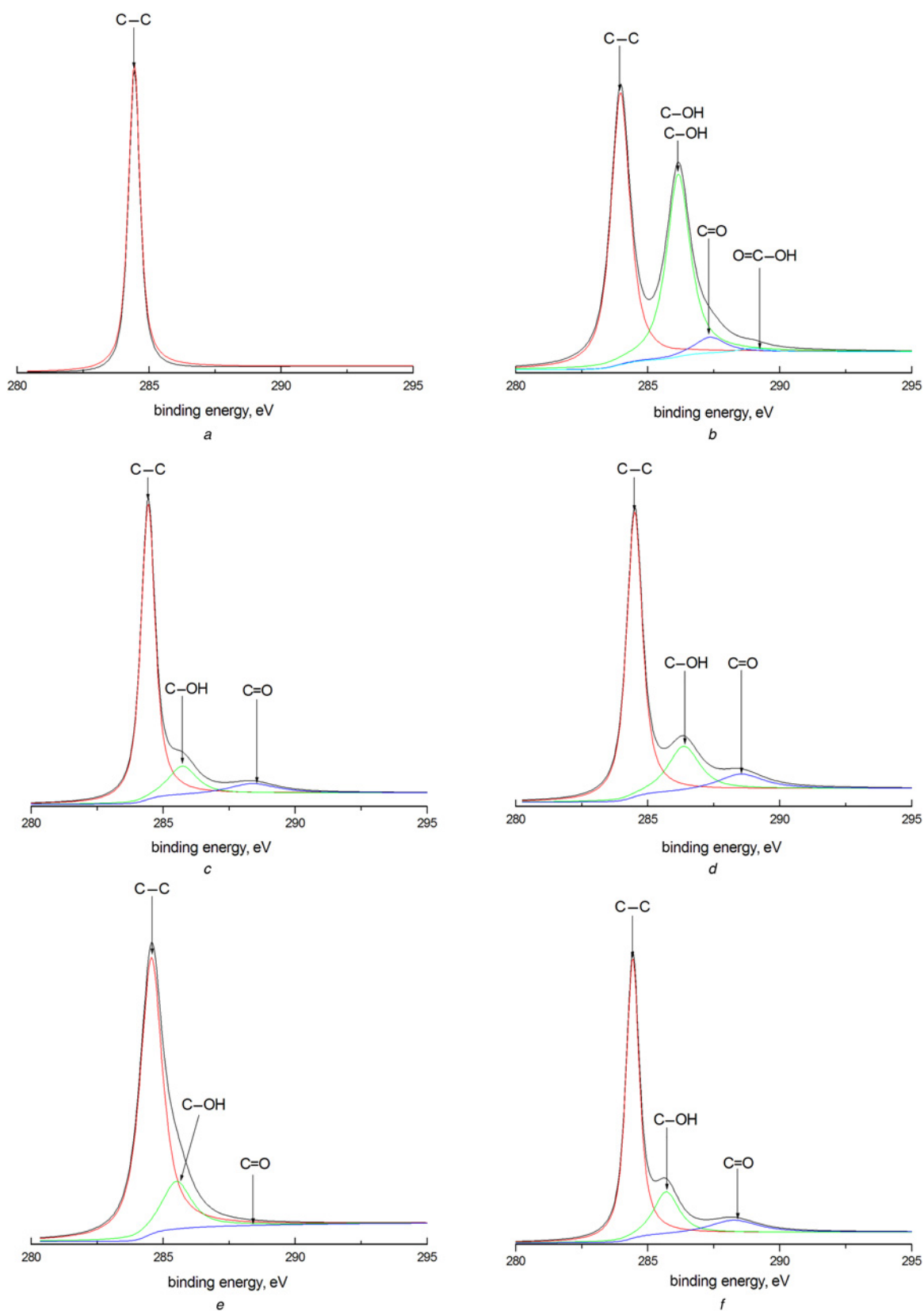


**Fig. 3** XPS spectra of  
*a* GRA  
*b* GO  
*c* RGO-1  
*d* RGO-2  
*e* RGO-3  
*f* RGO-4

**Table 1** Values of C1s/O1c (atomic ratios) obtained by XPS survey spectra

	GRA	GO	RGO-1	RGO-2	RGO-3	RGO-4
atomic ratio C1s/O1c	53.18	2.695	8.697	4.252	9.730	7.160

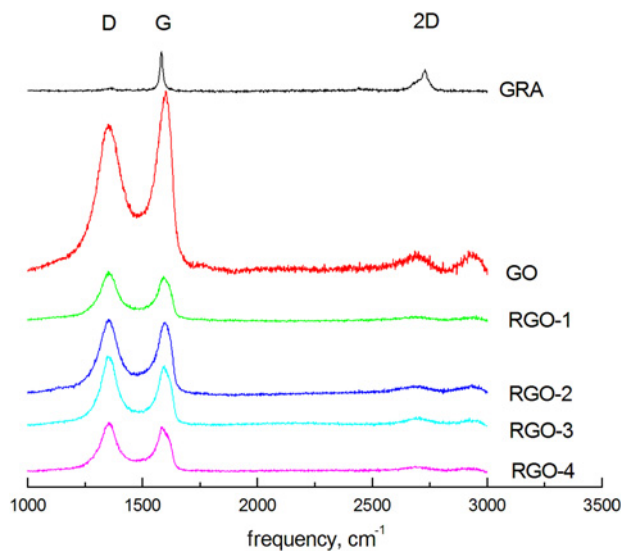


**Fig. 4** Raman spectra of GRA, GO, RGO-1, RGO-2, RGO-3 and RGO-4

**Table 2**  $I_D/I_G$  ratio of graphite (GRA), GO and RGOs

	GRA	GO	RGO-1	RGO-2	RGO-3	RGO-4
$I_D/I_G$	0.133	0.844	1.119	1.039	1.168	1.095

Vander Waals forces between layers by reducing with combination of hydrazine hydrate and HI.

3.6. Atomic force microscopy: The thickness of GO and RGO-3 was measured by AFM in tapping mode. As shown in Fig. 6, the thickness of GO and RGO-3 was about 7.358 and 0.656 nm,

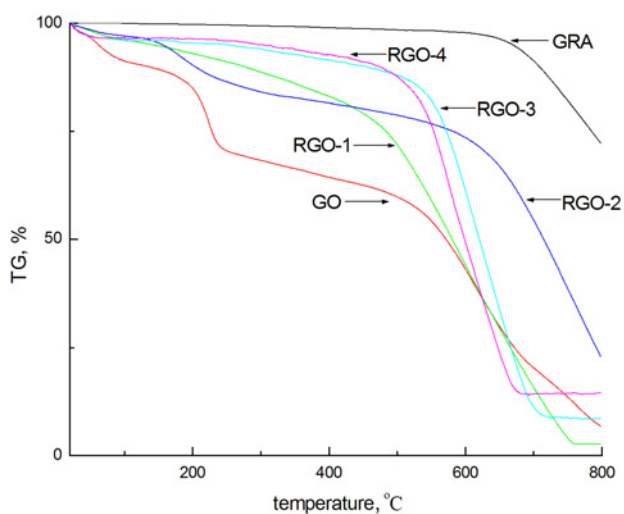


**Fig. 5** TGA spectra of GRA, GO, RGO-1, RGO-2, RGO-3 and RGO-4

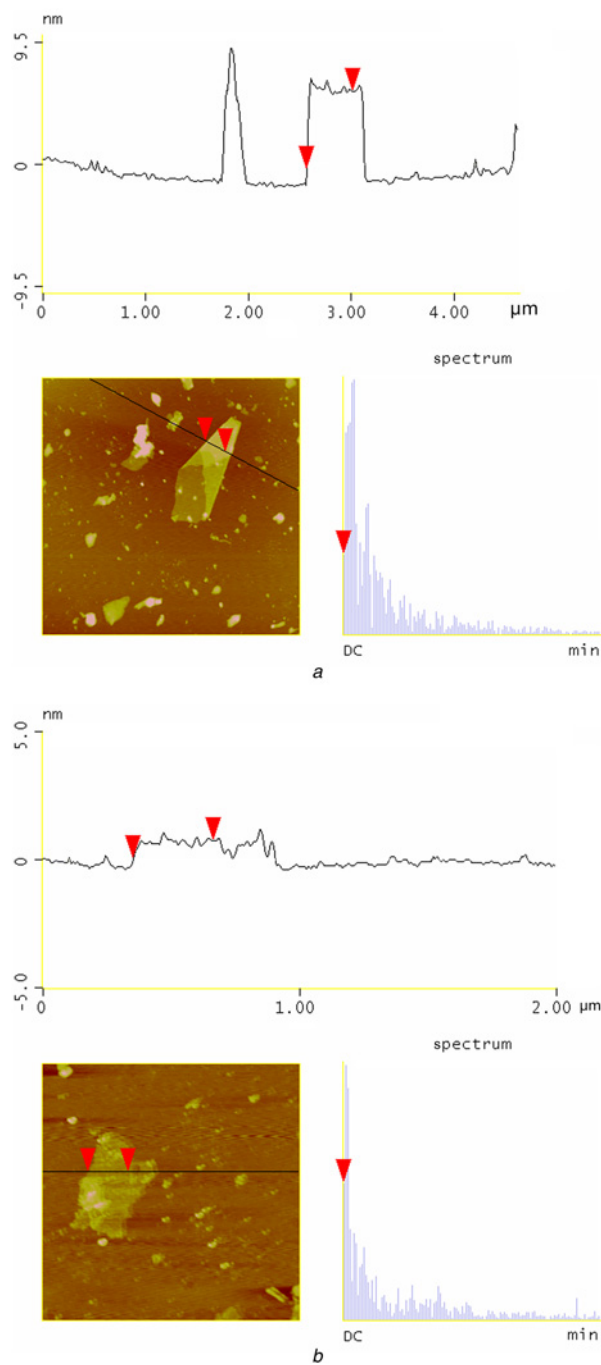


**Fig. 6** AFM spectra of  
a GO  
b RGO-3

respectively. The XRD results showed that the interlayer distances of GO and RGO-3 are 0.334 and 0.351 nm. It means that GO has about 22 layers and RGO-3 has about two layers.

3.7. Electrical conductivity: The electrical conductivities of GO and RGOs were measured by four-probe method with RTS-8 Four-probe tester. GO and RGO powders were pressed into a diameter of 13 mm, thickness of 0.3 mm thin wafer with powder tablet machine. The thin wafer was measured five times and the average values were recorded.

As shown in Table 3, the electrical conductivity of GO was about  $3.09 \times 10^{-4} \text{ S cm}^{-1}$ . The oxidation process introduced lots of oxygenated groups into the interlayer of graphite and destroyed the  $\pi$ - $\pi$

**Table 3** Electrical conductivity of GO and RGOs via different reducing reagents

	GO	RGO-1	RGO-2	RGO-3	RGO-4
electrical resistivity, $\Omega$ cm	$3.19 \times 10^3$	$3.56 \times 10^{-2}$	$2.23 \times 10^{-2}$	$1.25 \times 10^{-2}$	$3.24 \times 10^{-2}$
electrical conductivity, S $\text{cm}^{-1}$	$3.09 \times 10^{-4}$	28.09	44.91	79.89	30.89

conjugated structure of graphite. The electrical conductivity increased by five orders of magnitude when GO was reduced to RGO. The electrical conductivity of RGO-1, RGO-2, RGO-3 and RGO-4 were 28.09, 44.91, 79.89 and 30.89 S  $\text{cm}^{-1}$ , respectively. The oxygenated groups were removed and the  $\pi$ - $\pi$  conjugated structure was partly restored. The electrical conductivity of RGO-3 was much higher than other RGOs for more oxygenated groups were removed and the  $\pi$ - $\pi$  conjugated structure was restored better than others.

The characterisation results of RGO-3 clearly demonstrated that GO was reduced to bilayer graphene with the combination of hydrazine hydrate and HI. Majority of oxygenated functional groups was removed in RGO-3 after reduction process. The thermal stability and the atomic ratio (C1s/O1s) of RGO-3 from the XPS analyses are higher than other RGOs. This extensive reduction, along with a relatively small average interlayer distance as measured by XRD (3.51 Å), is probably the main reason for the higher electrical conductivity of RGO-3 reduced by combination of hydrazine hydrate and HI.

As we expected, combination of hydrazine hydrate and HI has shown good synergistic effect in GO reduction process. Hydrazine hydrate can reduce hydroxyl group easily at first, and then HI can remove epoxy functional group efficiently. Most of oxygenated functional group has been removed, the carbon skeleton was rebuilt, the thermal stability was restored, the atomic ratio (C1s/O1s) of RGO increased. The  $\pi$ - $\pi$  conjugated network structure was recovered; the electrical conductivity was higher than others.

RGO, which was reduced by combination of hydrazine hydrate and HI, was applied in polymer composites with polyaniline and polyvinyl alcohol in our next research. It can greatly improve the electrical conductivity and mechanical properties of polymer composites.

**4. Conclusions:** In conclusion, we use combination of hydrazine hydrate and HI as an efficient and convenient method to reduce GO to high-quality RGO nanosheets. The electrical conductivity of RGO-3 powder increased dramatically because of high degree of de-oxygenation and high graphitisation. This novel approach can be used for the fabrication and processing of bilayer graphene. As the conductive nanofiller, graphene has greatly improved the conductivity of polymer composites (PVA, PANI) in our recent work.

## 5 References

[1] Novoselov K.S., Geim A.K., Morozov S.V., *ET AL.*: 'Electric field effect in atomically thin carbon films', *Science*, 2004, **306**, pp. 666–669

[2] Kane C.L.: 'Materials science: erasing electron mass', *Nature*, 2005, **438**, pp. 168–170

[3] Lee C., Wei X., Kysar J.W., *ET AL.*: 'Measurement of the elastic properties and intrinsic strength of monolayer graphene', *Science*, 2008, **321**, pp. 385–388

[4] Chae H.K., Siberio-Pérez D.Y., Kim J., *ET AL.*: 'A route to high surface area, porosity and inclusion of large molecules in crystals', *Nature*, 2004, **427**, pp. 523–527

[5] Hirata M., Gotou T., Horiuchi S., *ET AL.*: 'Thin-film particles of graphite oxide 1: high-yield synthesis and flexibility of the particles', *Carbon*, 2004, **42**, pp. 2929–2937

[6] Reina A., Jia X., Ho J., *ET AL.*: 'Large area, few-layer graphene films on arbitrary substrates by chemical vapor deposition', *Nano Lett.*, 2008, **9**, pp. 30–35

[7] Stankovich S., Dikin D.A., Piner R.D., *ET AL.*: 'Synthesis of graphene-based nanosheets via chemical reduction of exfoliated graphite oxide', *Carbon*, 2007, **45**, pp. 1558–1565

[8] Choucair M., Thordarson P., Stride J.A.: 'Gram-scale production of graphene based on solvothermal synthesis and sonication', *Nat. Nanotechnol.*, 2008, **4**, pp. 30–33

[9] Hassan H.M., Abdelsayed V., Abd El Rahman S.K., *ET AL.*: 'Microwave synthesis of graphene sheets supporting metal nanocrystals in aqueous and organic media', *J. Mater. Chem.*, 2009, **19**, pp. 3832–3837

[10] Wang S., Tambraparni M., Qiu J., *ET AL.*: 'Thermal expansion of graphene composites', *Macromolecules*, 2009, **42**, pp. 5251–5255

[11] Cote L.J., Cruz-Silva R., Huang J.: 'Flash reduction and patterning of graphite oxide and its polymer composite', *J. Am. Chem. Soc.*, 2009, **131**, pp. 11027–11032

[12] Wu Z., Ren W., Gao L., *ET AL.*: 'Synthesis of graphene sheets with high electrical conductivity and good thermal stability by hydrogen arc discharge exfoliation', *ACS Nano*, 2009, **3**, pp. 411–417

[13] Pei S., Zhao J., Du J., *ET AL.*: 'Direct reduction of graphene oxide films into highly conductive and flexible graphene films by hydrohalic acids', *Carbon*, 2010, **48**, pp. 4466–4474

[14] Shin H.J., Kim K.K., Benayad A., *ET AL.*: 'Efficient reduction of graphite oxide by sodium borohydride and its effect on electrical conductance', *Adv. Funct. Mater.*, 2009, **19**, pp. 1987–1992

[15] Li D., Müller M.B., Gilje S., *ET AL.*: 'Processable aqueous dispersions of graphene nanosheets', *Nat. Nanotechnol.*, 2008, **3**, pp. 101–105

[16] Wang Z., Zhou X., Zhang J., *ET AL.*: 'Direct electrochemical reduction of single-layer graphene oxide and subsequent functionalization with glucose oxidase', *J. Phys. Chem. C*, 2009, **113**, pp. 14071–14075

[17] Zhang J., Yang H., Shen G., *ET AL.*: 'Reduction of graphene oxide via L-ascorbic acid', *Chem. Commun.*, 2010, **46**, pp. 1112–1114

[18] Fernandez-Merino M.J., Guardia L., Paredes J.I., *ET AL.*: 'Vitamin C is an ideal substitute for hydrazine in the reduction of graphene oxide suspensions', *J. Phys. Chem. C*, 2010, **114**, pp. 6426–6432

[19] Hummers W.S.Jr., Offeman R.E.: 'Preparation of graphitic oxide', *J. Am. Chem. Soc.*, 1958, **80**, p. 1339

[20] Cote L.J., Kim F., Huang J.: 'Langmuir-Blodgett assembly of graphite oxide single layers', *J. Am. Chem. Soc.*, 2008, **131**, pp. 1043–1049

[21] Park S., An J., Potts J.R., *ET AL.*: 'Hydrazine-reduction of graphite and graphene oxide', *Carbon*, 2011, **49**, pp. 3019–3023

[22] Dreyer D.R., Park S., Bielawski C.W., *ET AL.*: 'The chemistry of graphene oxide', *Chem. Soc. Rev.*, 2010, **39**, pp. 228–240

[23] Tuinstra F., Koenig J.L.: 'Raman spectrum of graphite', *J. Chem. Phys.*, 1970, **53**, pp. 1126–1130

[24] Ferrari A.C., Robertson J.: 'Interpretation of Raman spectra of disordered and amorphous carbon', *Phys. Rev. B*, 2000, **61**, p. 14095

[25] Tung V.C., Allen M.J., Yang Y., *ET AL.*: 'High-throughput solution processing of large-scale graphene', *Nat. Nanotechnol.*, 2008, **4**, pp. 25–29

[26] Jimenez P.S.: 'Thermal decomposition of graphite oxidation products DSC studies of internal combustion of graphite oxide', *Mater. Res. Bull.*, 1987, **22**, pp. 601–608